Published in final edited form as:
Science. 2013 June 28; 340(6140): 1587–1590. doi:10.1126/science.1237572.

B cells use mechanical energy to discriminate antigen affinities

Elizabeth Natkanski[1], **Wing-Yiu Lee**[1], **Bhakti Mistry**[1], **Antonio Casal**[1], **Justin E. Molloy**[2], and **Pavel Tolar**[1,*]

[1]Division of Immune Cell Biology, MRC National Institute for Medical Research, Mill Hill, London, UK

[2]Division of Physical Biochemistry, MRC National Institute for Medical Research, Mill Hill, London, UK

Abstract

The generation of high-affinity antibodies depends on the ability of B cells to extract antigens from the surfaces of antigen-presenting cells. B cells that express high-affinity B cell receptors (BCRs) acquire more antigen and obtain better T cell help. However, the mechanisms by which B cells extract antigen remain unclear. Using fluid and flexible membrane substrates to mimic antigen-presenting cells, we show that B cells acquire antigen by dynamic myosin IIa-mediated contractions that pull-out and invaginate the presenting membranes. The forces generated by myosin IIa contractions ruptured most individual BCR-antigen bonds and promoted internalization of only high-affinity, multivalent BCR microclusters. Thus, B cell contractility contributes to affinity discrimination by mechanically testing the strength of antigen binding.

Efficient antibody responses require selective expansion of B cell clones that recognize foreign antigens with high-affinity. B cells are initially stimulated by the binding of their B cell receptors (BCRs) to antigens on the surfaces of antigen-presenting cells (APCs) (1-5). During these cellular contacts, termed immune synapses, B cells acquire the antigens from the APCs (1, 2, 6), which leads to B cell antigen processing and presentation to helper T cells. The extent of T cell help, and resulting B cell activation, depends on the BCR affinity for antigen (7-9). Therefore, efficient affinity discrimination during antigen acquisition is essential for B cell clonal selection.

Although B cell synapse formation is sensitive to antigen affinity (10, 11), the mechanisms by which B cells extract antigens from APCs remain poorly understood (12, 13). To study this process, we developed an experimental model for studying immune synapses using immobilized plasma membrane sheets (PMS).

PMS are made from plasma membranes of adherent cells (14) and are suspended approximately 10 nm above the coverslip (Fig S1). Decoration of the exposed surfaces of PMS with antigens, but not with control proteins, induced B cell spreading and antigen clustering that resembled B cell synapses with planar lipid bilayers (PLB), an alternative model substrate (10, 15). However, unlike synapses with PLB, B cells rapidly internalized

*Correspondence to: ptolar@nimr.mrc.ac.uk.

One Sentence Summary B lymphocytes use myosin IIa contractility, coupled with clathrin-mediated endocytosis, as a specialized strategy to extract antigens from presenting surfaces in an affinity-dependent manner.

Supplementary Materials: Materials and Methods
Figures S1-8
Table S1
Movies S1-5

Europe PMC Funders Author Manuscripts

the antigen from synapses made with PMS (Fig. 1A, B, Movie S1). The ability of B cells to internalize antigen was not a result of the composition of the PMS, as PLB prepared from plasma membranes (PM-PLB) did not support antigen internalization (Fig. 1B). In addition, the internalization did not correlate with lipid or antigen diffusion within these substrates (Fig. S2).

To investigate why B cells internalize antigens from PMS, but not PLB, we examined the flexibility of these substrates using atomic force microscopy (AFM) and compared them to live APCs. In these experiments, the AFM tip binds to the substrate and then retracts to measure forces between the tip and the substrate until the rupture of the bond (16, 17). On PLB and PM-PLB, forces during tip retraction increased rapidly to 30-40 pN and produced single-step ruptures of bonds a few nanometers from the surface (Fig. 1C, D), indicating high membrane stiffness. In contrast, on both PMS and dendritic cells (DCs), forces initially increased and then plateaued at approximately 20 pN, with bonds often rupturing hundreds of nanometers away from the surface (Fig. 1C, D). Thus, in contrast to PLB or PM-PLB, PMS were flexible, and similar in their viscoelastic properties to plasma membranes of APCs loaded with physiological antigen complexes.

Labeling PMS with the hydrophobic dye, DiI, showed that B cells internalized antigen together with small pieces of the PMS membrane (Fig. 1A, E). We observed similar colocalization of antigen and lipid in B cells that acquired cognate immune complexes from DCs (Fig. 1E, F). In contrast, B cells forming synapses with PLB did not take up any DiI or antigen (Fig. 1A, E). These results resemble the acquisition of APC membranes by B cells in vivo (18), and, together with the force spectroscopy data, suggest that B cells require flexibility of the presenting membranes to pinch off the antigen together with the phospholipid bilayer.

To visualize the initiation of antigen extraction, we recorded TIRF timelapses of B cells interacting with the DiI-labeled PMS. Within a few seconds after B cell spreading, numerous spots of increased DiI fluorescence appeared in the PMS, and these spots continued to form and disappear dynamically (Fig. 2A, Movie S2). In contrast, DiI fluorescence remained diffuse in the absence of antigen (Fig. S3A). High-resolution 3D localization showed that the DiI spots were associated with upward movement of colocalized antigen particles (Fig. 2B, C). Thus, the increase in DiI fluorescence reports local lipid enrichment caused by antigen-induced B cell pulling-out and invaginating the presenting membranes.

Whereas antigen microclusters typically colocalized with a subset of membrane invaginations just before internalization (Fig. 2D), the membrane invaginations were more frequent and dynamic than antigen microclusters (Movie S3). Most invaginations lasted less than 5 s (Fig. 2E) and terminated abruptly (Fig. 2E, inset), suggesting physical rupture. Analysis of DiI and antigen fluorescence showed that the longer-lived invaginations started at sites that contained higher amounts of antigen compared to short-lived invaginations, and there was a significant drop in antigen fluorescence after their termination, indicating antigen internalization (Fig. 2F, Fig. S3B). These results show that B cells pulled-out the presenting-membranes at sites that contained variable amounts of antigen, but the lifetime of the invaginations and the probability of their internalization depended on prior formation of antigen microclusters.

To understand the mechanisms that regulate antigen internalization from the invaginations, we analyzed the dynamics of clathrin (19, 20). Following B cell spreading on PMS, the numbers of clathrin-coated structures (CCSs), and their brightness, increased compared to PMS without antigen (Fig. 2G, H). CCSs formed throughout the synapse, and we observed

simultaneous disappearance of long-lived invaginations, antigen microclusters and CCSs (Fig. S4). Short-lived invaginations rarely colocalized with CCSs, but 20% of long-lived invaginations colocalized with CCSs, particularly at the end of their lifetime (Fig. 2I). To assess the importance of CCSs in antigen acquisition, we knocked-down components of CCSs in Ramos B cells using shRNA. Knockdown of AP2 and dynamin2 inhibited antigen internalization from PMS (Fig. 3A), although pulling of membrane invaginations was not affected (Fig. 3B). These findings were confirmed in primary B cells using a dynamin2 inhibitor (Fig. 3C, D). Thus, CCSs pinch off invaginated antigen microclusters leading to internalization of the antigen. However, clathrin-independent mechanisms are required to first pull-out the presenting membrane.

Using shRNA-mediated knockdown and pharmacological inhibition, we found that myosin IIa and its activator, Rock1, were required for both membrane invagination and antigen internalization from PMS (Fig. 3A-D). In contrast, inhibition of myosin IIa did not prevent internalization of soluble antigen (Fig. 3C) or B cell spreading on the PMS (Fig. S5), suggesting that myosin IIa is not required for all BCR signaling or endocytosis. TIRF microscopy showed that myosin IIa formed dynamic spots and short fibers throughout the synapse (Fig. 3E, Movie S4) and specifically accumulated at the sites of membrane invaginations just before their onset (Fig. 3F). Myosin IIa then rapidly cleared from the center of growing invaginations, but remained closely associated with their sides (Fig. 3E-F). In contrast, F-actin accumulated at the onset of membrane invaginations, persisted throughout their lifetime, and disappeared after their termination (Fig. S6A-C, Movie S5). In longer-lived invaginations, a second wave of F-actin recruitment was detectable at the end of the invagination's lifetime (Fig. S6B, C). Together, these results show that B cells use acto-myosin contractility to pull-out and invaginate the presenting membranes, which is required to internalize the antigen via a clathrin- and actin-dependent process (21, 22). The observed short lifetime of most invaginations leads to a prediction that BCR-antigen bonds within small microclusters rupture under the pulling forces, aborting endocytosis. However, BCR-antigen interactions within larger microclusters resist the contractile forces for more than 20-30 s, allowing association or maturation of CCSs and internalization. This suggests that contractile forces mechanically test the strength of BCR binding immediately before internalization, providing a possible proofreading mechanism for affinity discrimination.

To extract antigen, BCR-antigen bonds would have to resist forces of up to 20 pN (Fig. 1D). To directly characterize the mechanical strength of individual BCR-antigen bonds, we measured BCR-antigen rupture forces using AFM force spectroscopy (Fig. 4A-C, Fig. S7). In these experiments, we varied the speed of cantilever retraction to subject the bonds to various bond-loading rates. This can reveal dependence of bond dynamics on applied forces (23). We conjugated AFM tips to NP or NIP antigens, which differ approximately 10 times in their 3D affinity for the B1-8 F_{ab} fragment (Table S1). Measurements of forces between NIP antigens and the B1-8 F_{ab} attached to coverslips, showed a sharp increase of force with cantilever retraction, resulting in single step ruptures (Fig. 4A, top). The mean rupture forces between the F_{ab} and the NP or NIP antigens rose linearly with the logarithm of the loading rates as expected (24) (Fig. 4B, C), and yielded extrapolated zero-force off-rates similar to those measured in solution (Fig. S7B). Force spectroscopy with living B1-8 B cells showed that forces between the B1-8 BCR and antigens also rose steadily with cantilever retraction (Fig. 4A, bottom), consistent with the BCR being anchored to the submembrane cytoskeleton (16, 25). Consequently, loading rates on the BCR were only modestly lower than on the F_{ab}. However, the rupture forces of the BCR-antigen bonds showed a non-linear dependence on the logarithm of loading rates (Fig. 4B, C). For slow loading rates, induced by pulling speeds similar to those generated by myosin IIa contractility, rupture forces for the BCR were lower, and had shorter lifetimes than those with the F_{ab}, suggesting that single BCR-antigen bonds break quickly at forces required for antigen extraction (Fig. S7D). Thus,

the mechanical strength of single BCR-antigen bonds is not sufficient for antigen extraction, highlighting the importance of load-sharing in multivalent BCR microclusters. In contrast, with faster loading rates, BCR-antigen rupture forces increased sharply and approached those measured with the F_{ab}. These data suggest that at higher forces, the BCR improves its resistance to mechanical stress, providing an additional layer of regulation.

What are the implications of these findings for antigen affinity discrimination? We found that B1-8 B cells internalized NP and NIP antigens to similar extent from solution (Fig. 4D). However, when the antigens were presented on PMS, B1-8 B cells internalized significantly more of the NIP antigen than the NP antigen (Fig. 4E). The NIP antigen also induced faster microcluster formation (Fig. S8A), longer lifetime of invaginations (Fig. 4F), and increased amounts of invagination-associated antigen (Fig. 4G). In addition, we found that although inhibition of myosin IIa by high concentration of blebbistatin abolished internalization of both antigens, modulation of the strength of myosin IIa contraction by low concentrations of blebbistatin reduced internalization of the NIP antigen, while it promoted the internalization of the NP antigen (Fig. 4H). This suggests reduced myosin IIa activity improves low-affinity BCR binding by reducing the mechanical stress on the bonds. Thus, the ability of B cells to discriminate between these two antigens depends on the strength of actomyosin-mediated force, implicating contractile forces in the regulation of affinity discrimination.

Due to the bivalency of the BCR and the multivalency of most physiologically relevant antigens, the half-lives of BCR-antigen complexes can reach many hours. As a result, B cells typically internalize soluble multivalent antigens in an affinity-independent manner (12). However, *in vivo*, B cells acquire multivalent antigens in an affinity-dependent manner (7, 18). We suggest that myosin IIa-generated forces shorten the lifetime of synaptic BCR-antigen bonds, promoting affinity discrimination on a physiologically relevant time-scale, i.e. seconds rather than hours. Since the initial growth of BCR microclusters is dependent on affinity (11) (Fig. S8A), higher-affinity antigens will form larger microclusters with higher number of bonds faster than lower-affinity antigens. When contractile forces engage, the higher number of bonds in larger microclusters, together with better resistance to force of the individual high-affinity bonds, will provide stability to the microclusters, allowing association with CCSs and endocytosis of the antigen. As a result, the probability of antigen internalization will depend on BCR affinity.

Spending mechanical energy to discriminate between interactions that could not be distinguished passively likely contributes to B cells' ability to develop high-affinity antibodies. This strategy seems to rely on mechanisms linking receptor signaling to myosin IIa contractility and endocytosis (26-28). Understanding of this process may inspire new ideas to improve antibody affinity beyond the nanomolar range, both in *in vivo* and *in vitro* affinity maturation systems.

Supplementary Material

Refer to Web version on PubMed Central for supplementary material.

Acknowledgments

We thank S. Martin for help with binding studies. B1-8$^{flox/flox}$ mice were a kind gift from K. Rajewsky, obtained under material transfer agreement with MGC Foundation. This work has been supported by Medical Research Council UK (Unit Programmes numbers U117597138 and U117570592).

References and Notes

1. Carrasco YR, Batista FD. B cells acquire particulate antigen in a macrophage-rich area at the boundary between the follicle and the subcapsular sinus of the lymph node. Immunity. 2007; 27:160–171. [PubMed: 17658276]
2. Phan TG, et al. Immune complex relay by subcapsular sinus macrophages and noncognate B cells drives antibody affinity maturation. Nat. Immunol. 2009; 10:786. [PubMed: 19503106]
3. Junt T, et al. Subcapsular sinus macrophages in lymph nodes clear lymph-borne viruses and present them to antiviral B cells. Nature. 2007; 450:110. [PubMed: 17934446]
4. Qi H, Egen JG, Huang AYC, Germain RN. Extrafollicular activation of lymph node B cells by antigen-bearing dendritic cells. Science. 2006; 312:1672–1676. [PubMed: 16778060]
5. Gonzalez SF, et al. Capture of influenza by medullary dendritic cells via SIGN-R1 is essential for humoral immunity in draining lymph nodes. Nat. Immunol. 2010; 11:427–434. [PubMed: 20305659]
6. Batista FD, Iber D, Neuberger MS. B cells acquire antigen from target cells after synapse formation. Nature. 2001; 411:489–494. [PubMed: 11373683]
7. Schwickert TA, et al. A dynamic T cell-limited checkpoint regulates affinity-dependent B cell entry into the germinal center. J. Exp. Med. 2011; 208:1243–1252. [PubMed: 21576382]
8. Victora GD, et al. Germinal center dynamics revealed by multiphoton microscopy with a photoactivatable fluorescent reporter. Cell. 2010; 143:592–605. [PubMed: 21074050]
9. Shih T-AY, Meffre E, Roederer M, Nussenzweig MC. Role of BCR affinity in T cell dependent antibody responses in vivo. Nat. Immunol. 2002; 3:570–575. [PubMed: 12021782]
10. Fleire SJ, et al. B cell ligand discrimination through a spreading and contraction response. Science. 2006; 312:738–741. [PubMed: 16675699]
11. Liu W, Meckel T, Tolar P, Sohn HW, Pierce SK. Antigen affinity discrimination is an intrinsic function of the B cell receptor. J. Exp. Med. 2010; 207:1095–1111. [PubMed: 20404102]
12. Batista FD, Neuberger MS. B cells extract and present immobilized antigen: implications for affinity discrimination. EMBO J. 2000; 19:513–520. [PubMed: 10675320]
13. Yuseff M-II, et al. Polarized secretion of lysosomes at the B cell synapse couples antigen extraction to processing and presentation. Immunity. 2011; 35:361–374. [PubMed: 21820334]
14. Moore MS, Mahaffey DT, Brodsky FM, Anderson RG. Assembly of clathrin-coated pits onto purified plasma membranes. Science. 1987; 236:558–563. [PubMed: 2883727]
15. Tolar P, Hanna J, Krueger PD, Pierce SK. The constant region of the membrane immunoglobulin mediates B cell-receptor clustering and signaling in response to membrane antigens. Immunity. 2009; 30:44–55. [PubMed: 19135393]
16. Evans E, Calderwood DA. Forces and bond dynamics in cell adhesion. Science. 2007; 316:1148–1153. [PubMed: 17525329]
17. Müller DJ, Helenius J, Alsteens D, Dufrêne YF. Force probing surfaces of living cells to molecular resolution. Nat. Chem. Biol. 2009; 5:383–390. [PubMed: 19448607]
18. Suzuki K, Grigorova I, Phan TG, Kelly LM, Cyster JG. Visualizing B cell capture of cognate antigen from follicular dendritic cells. J. Exp. Med. 2009; 206:1485–1493. [PubMed: 19506051]
19. Stoddart A, Jackson AP, Brodsky FM. Plasticity of B cell receptor internalization upon conditional depletion of clathrin. Mol. Biol. Cell. 2005; 16:2339–2348. [PubMed: 15716350]
20. Chaturvedi A, Martz R, Dorward D, Waisberg M, Pierce SK. Endocytosed BCRs sequentially regulate MAPK and Akt signaling pathways from intracellular compartments. Nat. Immunol. 2011; 12:1119–1126. [PubMed: 21964606]
21. Boulant S, Kural C, Zeeh J-C, Ubelmann F, Kirchhausen T. Actin dynamics counteract membrane tension during clathrin-mediated endocytosis. Nat. Cell Biol. 2011; 13:1124–1131. [PubMed: 21841790]
22. Cureton DK, Massol RH, Whelan SPJ, Kirchhausen T. The Length of Vesicular Stomatitis Virus Particles Dictates a Need for Actin Assembly during Clathrin-Dependent Endocytosis. PLoS Pathog. 2010; 6:e1001127. [PubMed: 20941355]

23. Dudko OK, Hummer G, Szabo A. Theory, analysis, and interpretation of single-molecule force spectroscopy experiments. Proc. Natl. Acad. Sci. U.S.A. 2008; 105:15755–15760. [PubMed: 18852468]
24. Bell GI. Models for the specific adhesion of cells to cells. Science. 1978; 200:618–627. [PubMed: 347575]
25. Treanor B, et al. The membrane skeleton controls diffusion dynamics and signaling through the B cell receptor. Immunity. 2010; 32:187–199. [PubMed: 20171124]
26. Vascotto F, et al. The actin-based motor protein myosin II regulates MHC class II trafficking and BCR-driven antigen presentation. J. Cell Biol. 2007; 176:1007–1019. [PubMed: 17389233]
27. Levayer R, Pelissier-Monier A, Lecuit T. Spatial regulation of Dia and Myosin-II by RhoGEF2 controls initiation of E-cadherin endocytosis during epithelial morphogenesis. Nat. Cell Biol. 2011; 13:529–540. [PubMed: 21516109]
28. Kuo J-C, Han X, Hsiao C-T, Yates JR, Waterman CM. Analysis of the myosin-II-responsive focal adhesion proteome reveals a role for β-Pix in negative regulation of focal adhesion maturation. Nat. Cell Biol. 2011; 13:383–393. [PubMed: 21423176]
29. Ehrlich M, et al. Endocytosis by random initiation and stabilization of clathrin-coated pits. Cell. 2004; 118:591–605. [PubMed: 15339664]
30. Riedl J, et al. Lifeact: a versatile marker to visualize F-actin. Nat. Methods. 2008; 5:605–607. [PubMed: 18536722]
31. Wu M, et al. Coupling between clathrin-dependent endocytic budding and F-BAR-dependent tubulation in a cell-free system. Nat. Cell Biol. 2010; 12:902–908. [PubMed: 20729836]
32. Sund SE, Swanson JA, Axelrod D. Cell membrane orientation visualized by polarized total internal reflection fluorescence. Biophys. J. 1999; 77:2266–2283. [PubMed: 10512845]
33. Anantharam A, Axelrod D, Holz RW. Real-time imaging of plasma membrane deformations reveals pre-fusion membrane curvature changes and a role for dynamin in the regulation of fusion pore expansion. J. Neurochem. 2012; 122:661–671. [PubMed: 22671293]
34. Huang B, Wang W, Bates M, Zhuang X. Three-dimensional super-resolution imaging by stochastic optical reconstruction microscopy. Science. 2008; 319:810–813. [PubMed: 18174397]
35. Dudko OK, Hummer G, Szabo A. Intrinsic rates and activation free energies from single-molecule pulling experiments. Phys. Rev. Lett. 2006; 96:108101. [PubMed: 16605793]
36. Friddle RW, Noy A, De Yoreo JJ. Interpreting the widespread nonlinear force spectra of intermolecular bonds. Proc. Natl. Acad. Sci. U.S.A. 2012; 109:13573–13578. [PubMed: 22869712]

Europe PMC Funders Author Manuscripts

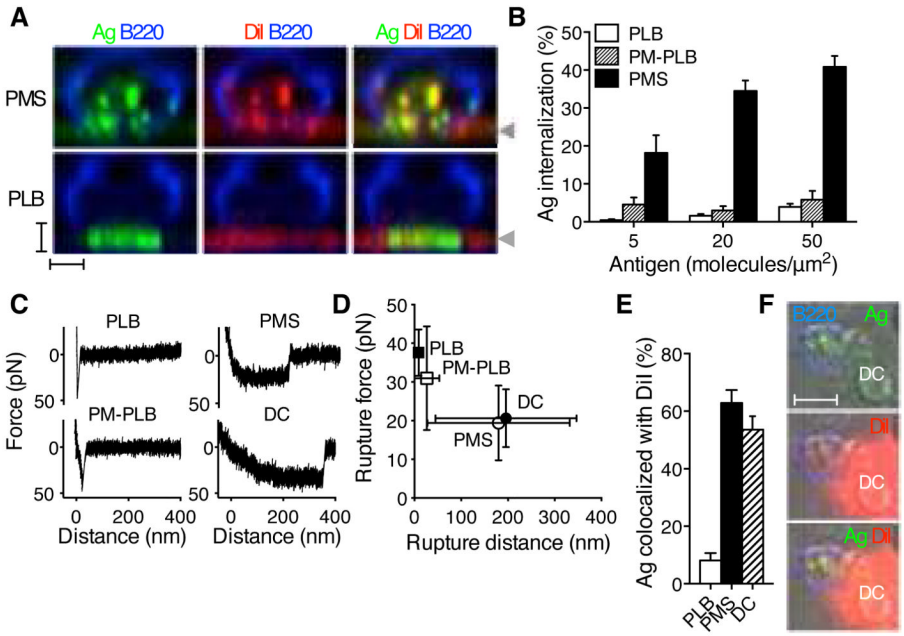

Fig. 1.

B cells acquire antigens from flexible membranes. (**A**) Sideview reconstruction of B220-stained primary B cells forming synapses with DiI-stained and anti-Igκ antigen-loaded (Ag) PMS or PLB. Arrowheads indicate the position of the substrate. Scalebars, 2 μm. (**B**) Image quantification of primary B cell antigen internalization (means±SEM, n=23-60 cells). (**C**) AFM force retraction curves of streptavidin-coated AFM tip and biotinylated antigens. Antigens were anti-Igκ for PLB, PM-PLB and PMS, and immune complexes of NIP antigen for DCs. Speed of retraction was 0.1μm/s. (**D**) Rupture distances and forces, mean±SD, n=31-109 retraction curves. (**E**) Colocalization of internalized antigen with DiI in primary B cells after internalization from the substrates. Means±SEM, n=12-21 cells. (**F**) B220-stained B1-8 primary B cell internalizing immune complexes of NIP antigen from a DC stained with DiI. Scalebar, 5 μm.

Europe PMC Funders Author Manuscripts

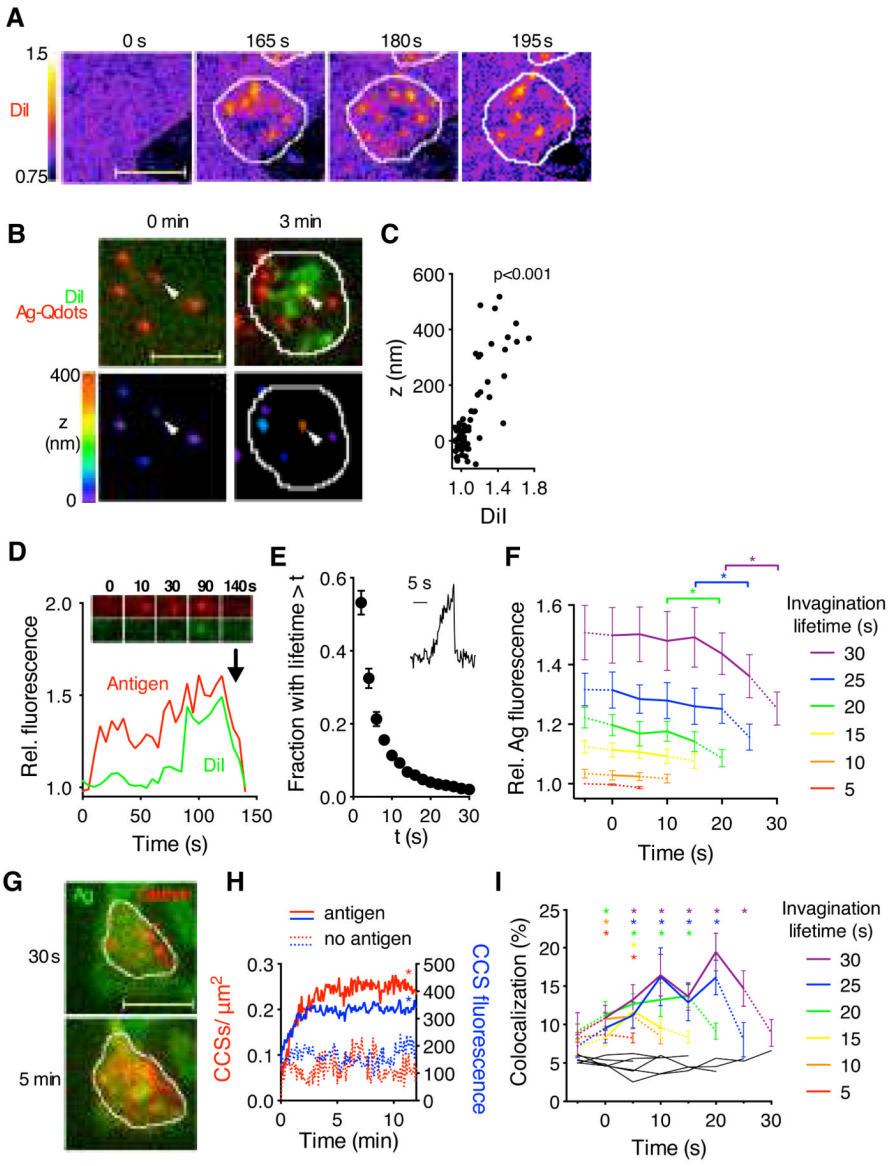

Fig. 2.

Primary B cells extract antigens by invaginating and pinching off the presenting membranes. (**A**) Changes in DiI intensity on antigen-loaded PMS after B cell spreading (white outline). (**B**) 3D localization of antigen. Top, DiI-stained PMS loaded with unlabeled antigen and antigen-Qdots before and after B cell spreading. Bottom, antigen-Qdots color-coded for their vertical position. Arrowhead shows a Qdot pulled-up by the B cell. (**C**) Vertical position of antigen-Qdots versus colocalized DiI fluorescence (n=10 cells, p for Pearson correlation test). (**D**) Antigen and DiI fluorescence in a single antigen microcluster. Arrow indicates internalization. (**E**) Lifetimes of invaginations (mean±SEM, n=7 cells). Inset, DiI fluorescence of a short-lived invagination. (**F**) Antigen fluorescence in invaginations grouped by lifetime. Dotted lines show fluorescence before and after invagination's lifetime (mean±SEM, n=10 cells). *, $p<0.01$ in paired t-tests. (**G**) B cell expressing clathrin light chain-GFP spreading on antigen-loaded PMS. (**H**) Numbers and fluorescence of synaptic CCSs (mean±SEM, n=15-21 cells, *, $p<0.05$ in nonparametric tests for t>1 min against controls). (**I**) Percentage of invaginations colocalizing with CCSs (mean±SEM, n=12 cells).

Europe PMC Funders Author Manuscripts

Black lines, colocalization with randomly scrambled CCSs. *, $p<0.01$ in nonparametric tests against scrambled controls. Scale bars, 5 μm.

Europe PMC Funders Author Manuscripts

Europe PMC Funders Author Manuscripts

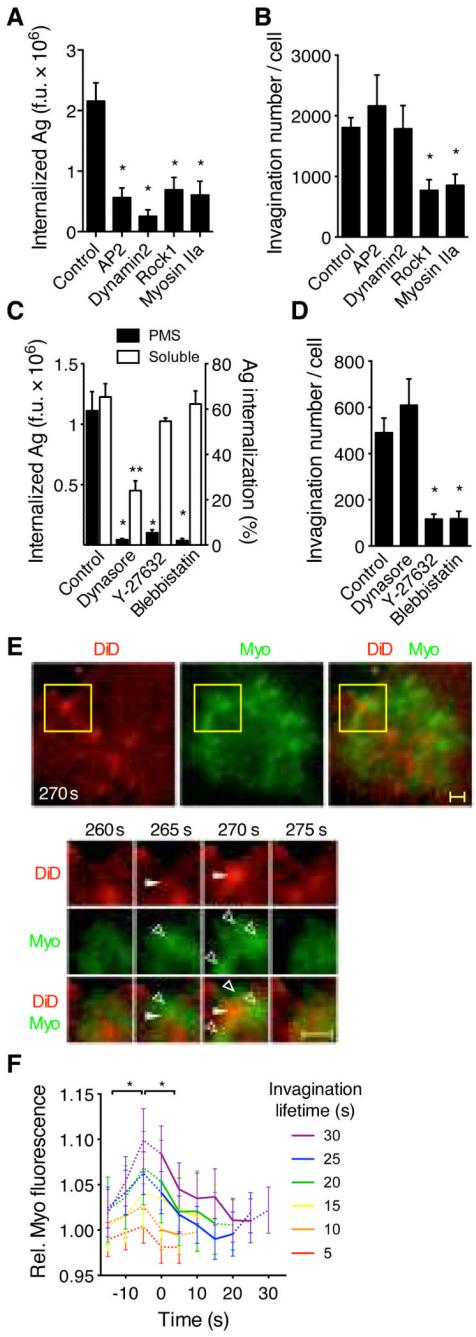

Fig. 3.

B cell antigen extraction requires myosin IIa contractility and clathrin-mediated endocytosis. (**A**) Antigen internalization (anti-Igμ) and (**B**) number of invaginations pulled from PMS by Ramos B cells expressing shRNA against AP2, dynamin2, Rock1, or myosin IIA. (**C**) Antigen internalization (anti-Igκ) from PMS (left y-axis) or solution (right y-axis) by primary B cells treated with inhibitors against dynamin2 (dynasore), Rock1 (Y-23632), or myosin IIA (blebbistatin). (**D**) Number of invaginations pulled from PMS by primary B cells treated with inhibitors. A-D, means±SEM, n=17-25 cells for internalization from PMS, n=7-15 cells for invagination numbers, n=3 experiments for soluble antigen internalization. *, $p<0.01$, **, $p<0.05$ in non-parametric tests against controls. F.u., fluorescence units. (**E**)

Top, TIRF image of a primary B cell expressing myosin IIa regulatory light chain (RLC)-GFP (Myo) spread on DiD-labeled PMS loaded with antigen. Yellow squares show a region magnified below. Closed arrowheads show invagination, open arrowheads show myosin IIa structures. Scalebar, 1 μm. (**F**) Quantification of myosin IIa RLC fluorescence in invaginations grouped by lifetime (mean±SEM, n=15 cells). *, $p<0.01$ in paired t-tests.

Europe PMC Funders Author Manuscripts

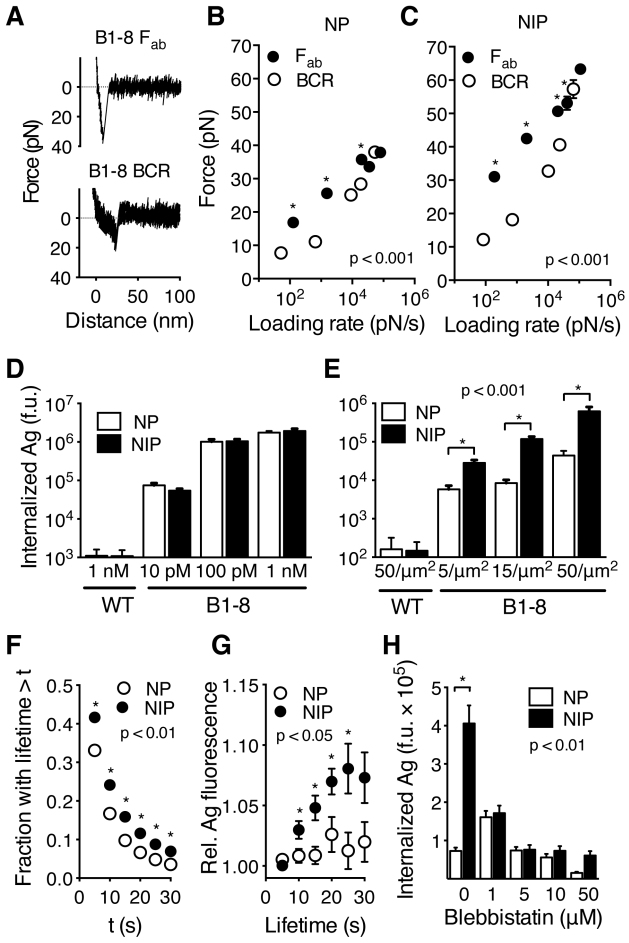

Fig. 4.

Forces generated by myosin IIa contractility promote affinity-dependent antigen internalization. (**A**) Force spectroscopy retraction curves showing rupture of bonds between NIP antigen and B1-8 F_{ab} fragment (top) or B1-8 BCR on live primary B1-8 B cells (bottom). Speed of retraction was 0.1 μm/s. (**B, C**) Mean rupture forces (±SEM) measured by AFM force spectroscopy with NP (**B**) and NIP (**C**) binding to B1-8 F_{ab} fragment on coverslips or to B1-8 BCR on B cells. Retraction speeds were 0.1-50 μm/s. N=41-185 retraction curves. (**D, E**) Internalization of antigens by B1-8 or wild type (WT) primary B cells from solution (D) or from PMS (E). (**F**) Lifetime of invaginations. (**G**) Antigen fluorescence associated with invaginations of indicated lifetime. (**H**) Internalization of antigens by B1-8 B cells treated with blebbistatin. D-H, means±SEM of individual cells, n=25-118. If error bars are not visible, they are smaller than the symbols. Asterisks show statistical significance in non-parametric tests at the indicated p-values.

Europe PMC Funders Author Manuscripts